Polymer 51 (2010) 1926–1933

Contents lists available at ScienceDirect

Polymer

journal homepage: www.elsevier.com/locate/polymer

Synthesis and biocompatibility of anionic polyurethane nanoparticles coated with adsorbed chitosan

Dan Xu [a,b,c], Ke Wu [d], Qiuhong Zhang [b,c], Heyi Hu [b], Kai Xi [b], Qingming Chen [a,b], Xuehai Yu [b], Jiangning Chen [d,**], Xudong Jia [a,b,c,*]

[a] State Key Laboratory of Coordination Chemistry, Nanjing University, Nanjing 210093, P. R. China
[b] Department of Polymer Science and Engineering, Nanjing University, Nanjing 210093, P. R. China
[c] Nanjing National Laboratory of Microstructures, Nanjing University, Nanjing 210093, P. R. China
[d] State Key Laboratory of Pharmaceutical Biotechnology, Department of Biochemistry, Nanjing University, Nanjing 210093, P.R. China

ARTICLE INFO

Article history:
Received 3 September 2009
Received in revised form
16 January 2010
Accepted 1 March 2010
Available online 9 March 2010

Keywords:
Waterborne polyurethane
Chitosan
Biocompatible

ABSTRACT

Through the assembly of polyelectrolyte in aqueous emulsion, we synthesized a series of core–shell ionic complex nanoparticles containing anionic polyurethane (PU) and cationic chitosan (CS). The physicochemical properties of PU–CS ionic complex (PU-c-CS) materials were investigated by IR, XPS, DLS, TEM, AFM, general tensile tests, and surface contact angle measurement. It was found that the sizes of the prepared nanoparticles were in the range from 60 to 220 nm, and the films exhibited good mechanical properties. The cell (HUVECs) culture experiments showed that the PU-c-CS films exhibited very low cytotoxicity and supported cell adhesion and growth. Protein (BSA) adsorption was significantly decreased for the PU-c-CS films. Furthermore, the results of prothrombin time (PT) and activated partial thromboplastin time (APTT) indicated that antithrombogenicity of the materials were effectively improved.

1. Introduction

Polyurethane block copolymers (PU) are widely used as cardiovascular biomaterials due to their excellent mechanical properties and good biocompatibility [1–3]. However, surface-induced thrombosis, protein adsorption, and cytocompatibility are three serious aspects when PU is used as implantable material [4,5]. And the intrinsic inert property of PU is unfavorable of endothelial cells growth [3]. Hence, it is necessary that PU would be modified to enhance antithrombogenicity and biocompatibility. Many approaches have focused on material surfaces because the hemocompatibility and cytocompatibility are mostly modulated by the surface of the materials, whilst the bulk physicochemical properties of the materials are rarely changed [6–10]. It has been reported that the immobilization of natural materials like gelatin, collagen, chitosan (CS), alginate or biotin, etc., onto the surface of polymeric materials helped to improve the biocompatibility of these materials [11–16].

Chitin [17], one of the most abundant naturally occurring polysaccharide, is a linear polymer consisting of *N*-acetyl-D-glucosamine units joined by β(1,4)-glycosidic linkages. Chitosan, chitin's deacylated derivative, exhibits much higher reactivity, many interesting physicochemical and biological properties [18,19]. Due to its biocompatibility, biodegradability and bioactivity, it is considered as a very interesting substance for diverse applications in biomaterials [20–23]. One of the CS's most promising features is its excellent ability for cell transplantation and tissue regeneration when it is incorporated into porous structure materials [24–27]. But CS has poor mechanical properties, and is difficult to be directly used.

Currently, many efforts have been applied to modify PU with natural CS for the preparation of new biomaterials with excellent mechanical property, good biocompatibility, increasing anticoagulation effect, and so on [3,15,16]. Zhu et al. [3] reported that the swollen CS was used as an extender for the preparation of modified PU through the co-polymerization; Lin et al. [15] immobilized CS onto the PU surface grafted with poly(acrylic acid); Yang et al. [16] studied impregnated CS onto the surface of PU fragment through *N*-isopropyl acrylamide and glutaraldehyde. The modified PU materials obtained by the reported methods were limited to be applied owing to the processing and moulding difficulties.

In this paper, novel biomaterials were synthesized by immobilizing CS onto the surface of waterborne PU through the assembly

* Corresponding author. State Key Laboratory of Coordination Chemistry, Nanjing University, Nanjing 210093, P. R. China. Tel.: +86 25 8359 4342; fax: +86 25 8359 6239.
** Corresponding author. Tel.: +86 25 8359 6796; fax: +86 25 8332 4605.
E-mail addresses: jnchen@nju.edu.cn (J. Chen), jiaxd@nju.edu.cn (X. Jia).

0032-3861/$ – see front matter © 2010 Elsevier Ltd. All rights reserved.
doi:10.1016/j.polymer.2010.03.008

of polyelectrolyte in aqueous emulsion. First, PTMO, IPDI, DMPA and TEA were used for the synthesis of the novel waterborne anionic PU. Then, a series of core–shell structure PU–CS ionic complex (PU-c-CS) aqueous emulsion would be formed when cationic CS solution was dropped into anionic PU aqueous emulsion through ionic complexation under very mild conditions. The biocompatibility of PU-c-CS films was examined by using cell culture experiments, protein adsorption assay, prothrombin time (PT) and activated partial thromboplastin time (APTT). The results indicated that the PU-c-CS films exhibited very low cytotoxicity and supported cell adhesion and growth while retaining good mechanical properties. In addition, the APTT was significantly prolonged and protein adsorption was obviously decreased for surface-modified PU-c-CS films. The results suggested that the novel PU-c-CS films would be very useful for practical applications of implantable materials.

2. Experimental section

2.1. Materials

CS with 90% degree of deacetylation and average molecular weight of 5000 was purchased from Yuhuan Ocean Biochemical Co. (Taizhou, China). Polytetramethylene oxide glycol (PTMO, Mn = 1000), isophorone diisocyanate (IPDI), 2,2′-dimethylol propionic acid (DMPA) were obtained from Sigma–Aldrich (USA) and dried under vacuum before use. Acetone and triethylamine (TEA) were purchased from Shanghai Chemical Co. (China) and purified by distillation. Other chemicals, including phosphate buffered saline (PBS), bovine serum albumin (BSA), sodium dodecyl sulfate (SDS) and dimethyl sulfoxides (DMSO) were of analytical grade and purchased from Sigma–Aldrich.

2.2. Preparations of PU-c-CS nanoparticles and films

PU copolymer made of PTMO, IPDI and DMPA was first synthesized by using a bulk polymerization procedure. IPDI (6.66 g) was firstly added into a polymerization flask containing PTMO (10.0 g) and the mixture was stirred at 80–85 °C for 3 h with a stirring rate of 350–400 rpm. DMPA (1.34 g) was then added to the flask and reacted for another 2 h under the same condition. The prepolymer was dissolved in 25 mL acetone, and ionized with TEA (1.01 g) for 10 min. Afterwards, the above copolymer emulsion was dropwise added into 50 mL distilled water under moderate stirring at room temperature overnight [28].

The resulting anionic PU copolymer was dispersed in mixed solvent (25 mL of acetone and 100 mL of distilled water). Acetone and redundant TEA were removed under reduced pressure by rotatory evaporator and the final volume of the aqueous emulsion was concentrated to about 60 mL at 25 °C.

PU-c-CS nanoparticles were easily prepared through ionic complexation reactions between PU aqueous emulsion and CS solution (1.62% wt), mixed in the volume ratio of 1:0.5, 1:1 and 1:2, respectively. The aqueous emulsion was stirred at 25 °C for 12 h. PU-c-CS aqueous emulsion was cast into Teflon disk and kept at 60 °C under vacuum in order to obtain dry PU-c-CS films. A total of 600 μL of PU-c-CS aqueous emulsion was added in each Petri dish, making it soak around the bottom. The solvent was evaporated in air and then in vacuum at room temperature.

2.3. Characterization

Infrared spectra (IR) were recorded with a Nicolet 5DX Fourier transform infrared spectrometer using films as samples.

The chemical composition of PU-c-CS film surface was determined by X-ray photoelectron spectroscopy (XPS). The XPS measurements were made on the Thermo ESCALAB 250 spectrometer (USA) with a monochromatized A1Ka X-ray source (1486.6 eV photos) at a constant dwell time of 100 ms and pass energy of 20 eV. The anode voltage and current were set at 15 kV and 10 mA, respectively. The samples were mounted on the sample stubs by double-sided adhesive tapes. The charging shift was referred to the C_{1s} line emitted from the saturated hydrocarbon [29]. Before the XPS measurements, the films were placed in tubes filled with distilled water for 48 h. Afterwards, the films were taken out and rinsed carefully by deionized water, then dried under vacuum.

The mean particle size and ξ-potential of the samples were determined, respectively, by BI-9000AT dynamic light scattering instrument (DLS) and Zetaplus potential analyzer (Brookhaven Instruments Corporation, New York, USA). All measurements were repeated for three times for each sample at room temperature.

Transmission electron microscopy (TEM) experiments were conducted on a JEM-1005 TEM (JEOL Co. Japan). In a typical experiment, one drop of the diluted emulsion sample was put to carbon film supported by a copper grid.

Atomic force microscopy (AFM) (SPI3800, Seiko Instruments Inc., Japan) was used to study the surface morphology of the films. One drop of properly diluted emulsion sample was placed on the surface of a clean silicon wafer and dried at 60 °C under vacuum. The AFM observations were performed with a 20 μm scanner in tapping mode.

The mechanical properties were determined on a table model Instron Series IX Automated Materials Testing System with Interface type of 4200. An ASTM 1708 standard die was used for the samples, which were dried under a vacuum for a minimum of 48 h before testing. The index was as follows: sample rate: 2.0 pts/s; crosshead speed: 20.0 mm/min; full scale load range: 0.50 KN; humidity: 60%; and temperature: 15 °C.

Water contact angle measurements were made by CAM 200 (KSV Instrument Ltd., Finland) at room temperature. The data were collected 1 min after the 6.5 μL drop of double-distilled water had been placed on the surface of the film. Results were presented as the average of at least 10 measurements on three different surfaces.

2.4. Hydrolytic stability of the samples

The samples were weighed (W_1) and placed in tubes filled with phosphate buffer (pH 7.4) in triplicate. The tubes were placed in the thermostatic shaker at 37 °C for 48 days. The samples were taken out and washed with distilled water, then dried at room temperature and weighed (W_2). The hydrolytic loss weight was calculated as follows [30].

$$\text{Loss weight(LW)} = (W_1 - W_2)/W_1 \times 100\%$$

The films had been placed in deionized water at 37 °C for 48 days and rinsed well by deionized water in triplicate. The pre-weighed dry specimens were immersed in deionized water at 25.0 °C. After equilibrating for 24 h, the samples were blotted with laboratory tissue and weighed. The water-swelling ratio (SR) was expressed as the weight percentage of water in the swollen sample.

$$\text{Swelling ratio(SR)} = (W_S - W_D)/W_D \times 100\%$$

Where W_S is the weight of the swollen sample, and W_D is the weight of the dry sample.

2.5. Cells culture and morphology observation

Human umbilical vein endothelial cells (HUVEC, ECV304) were used for the cell attachment and proliferation study. ECV304 cells

were routinely grown and maintained in RPMI-1640 medium containing 10% fetal bovine serum (FBS) and 100 U/mL penicillin and 100 mg/mL streptomycin. Two milliliter of cell suspension at a given density was placed on each Petri dish, pre-laid with PU or PU-c-CS films which were rinsed carefully with PBS and sterilized by UV-radiation, and maintained in a humidified atmosphere with 5% CO_2 at 37 °C. Blank dishes were used as control. Cell numbers were quantified every 12 h using a hemocytometer after exposure to trypsin/EDTA (Invitrogen, USA). And the cell proliferation was measured using the procedure of MTT reduction for cell viability measurement [16,31]. In brief, the medium was carefully removed from the cultured well and the floating cells were harvested at determined time points. The wells were washed with PBS, and 400 μL of medium containing the collected floating cells was added to the well. One milliliter of MTT-solution (1 mg/mL in PBS) was added to each well in the dark. The culture dish was packed with aluminum foil paper and incubated 4 h at 37 °C. The cultured medium was then removed by pipette, and 1 mL DMSO was added to each well and kept at room temperature for 30 min. Then, 100 μL mixed solution was transferred from each well into a 96-well culture dish. The solution of the well was examined with ELISA reader (Safire, Tecan, Switzerland) at 570 nm (reference wavelength: 655 nm).

Inverted microscopy (ECLIPSE TE2000, Nikon Co.) was used to take photos of randomly selected areas of the cultured cells every 12 h after ECV304 cells were plated. Blank Petri dish and PU film were used as control groups.

2.6. Protein adsorption assay

Protein adsorption assay was performed by adding 1 mL of BSA solution (3 mg/mL in PBS) on each Petri dish in triplicate. After 12 h of incubation in a humidified air containing 5% CO_2 at 37 °C, BSA solution was taken out, and the dishes were rinsed carefully with PBS. Then 1 ml of 2% SDS solution was added into each dish, followed by another 8 h of incubation. A protein analysis kit (micro-BCA protein assay regent kit, Shenergy Bioclor Co., China) based on the bicinchoninic acids (BCA) method was used to determine the concentration of BSA in the SDS solution [32,33].

2.7. Blood coagulation assays

A series of clean tubes were coated with emulsion and dried in octuple. Fresh rabbit blood (0.1 mL) containing sodium citrate and a solution of $CaCl_2$ (0.025 mol/L, 20.1 mL) were added into each tube. The time of the emergence of a milky white flocculate was recorded as the recalcification time (RT). Blank tubes and the tubes coated with silicon oil (SO) were used as control groups.

Five milligrams of samples was added into the tubes with 0.2 mL of 3.8% sodium citrate solution, and blank without sample added was used as control. Human whole blood (30 mL) from a healthy volunteer was collected, and 1 mL of the human whole blood was immediately added into these tubes. Then the human whole blood was centrifuged at 1000 rpm for 20 min at 4 °C to separate the blood corpuscles, and obtain the platelet-poor plasma (PPP) for blood coagulation time test. A sample was incubated 37 °C for 1 h. The APTT and PT of the PPP were determined by an automated blood coagulation analyzer (Helena Laboratories, USA) in triplicate [34,35].

2.8. Statistical analysis

The results were analyzed statistically using student's *t*-test to determine whether there were any statistically significant differences among the experimental groups at the 5 percent level of significance ($P < 0.05$). Results were expressed as mean values ± standard deviation (SD).

3. Results and discussion

3.1. Characterization of PU-c-CS

PU-c-CS nanoparticles were synthesized through the assembly of polyelectrolyte in aqueous emulsion. The preparation process of PU-c-CS nanoparticles was illustrated in Fig. 1 and the composition of each sample was summarized in Table 1. IR studies were conducted to investigate the complex formation between PU and CS. Fig. 2 showed the IR spectra of CS, PU and PU-c-CS films. CS is a positively charged polymer and easily forms ionic complex with anionic polymer [36,37]. In pure CS, amide band I at 1632 cm^{-1} and amide band II at 1554 cm^{-1} could be observed and bending and rocking vibration of $-CH_2$ appeared at 1412 cm^{-1}. The main characteristic bands for urea groups of pure PU and PU-c-CS were observed around 1700 cm^{-1} (C═O axial deformation) and 1543–1462 cm^{-1} (NH angular deformation) [1]. Compared with the spectra of CS and PU, the C═O stretching vibration of $-COO^-$ groups in PU-c-CS appeared at 1647 cm^{-1}. On the other hand, the broad absorption around 2472 cm^{-1} was attributed to the $-NH_3^+$ groups in PU-c-CS. These results indicated that the carboxylic groups of PU were dissociated into $-COO^-$ groups which complexed with protonated amino groups of CS through electrostatic interaction to form the polyelectrolyte complex during the emulsion polymerization procedure.

Surface composition was analyzed by XPS. Fig. 3 showed the XPS spectra of CS, PU and PU-c-CS films. All binding energy data were reproducible within ±0.2 eV. The spectra of PU film showed three carbon, one oxygen and two nitrogen peaks while CS and the

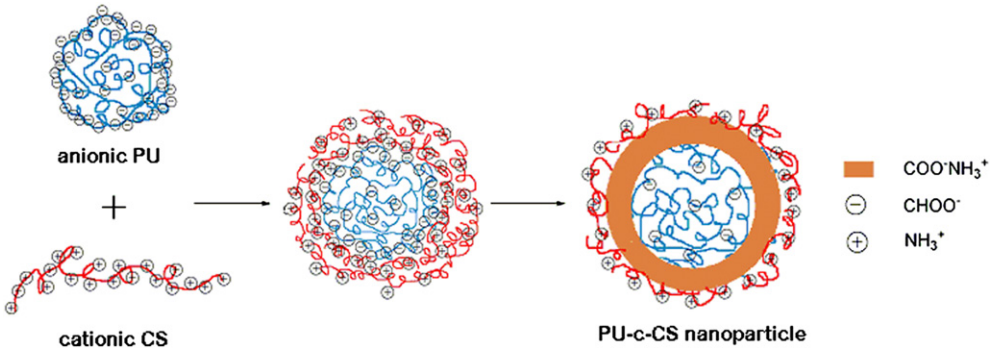

Fig. 1. Illustration of the preparation process of biocompatible PU-c-CS nanoparticle.

Table 1
Summarization of sample composition.

Sample	CS content (g)	Ratio of n_{CS}:n_{PU}
PU	0	
PU-c-CS1	0.81	1:2
PU-c-CS2	1.62	1:1
PU-c-CS3	3.24	1:0.5

n_{CS} is the molar number of amino group in CS; and n_{PU} is the molar number of carboxyl group in PU.

PU-c-CS films showed four carbon, two oxygen and two nitrogen peaks. The C_{1s} peak corresponding to the aliphatic and aromatic carbons was observed at 285.0 eV [2]. The C_{1s} peaks for amino and ethereal carbon were located at 286.0 and 286.5 eV, respectively. The C_{1s} peaks corresponding to the carbonyl and amide groups were observed at 288.0 and 288.2 eV, respectively. The C_{1s} peaks for ester, carboxylic acid and urea (carbonyl of the urethane groups) were all observed at 289.0 eV. The O_{1s} peaks corresponding to the oxygen of the carbonyl, hydroxyl and ester appeared at 532.2, 532.8 and 533.7 eV, respectively. The N_{1s} peaks corresponding to the nitrogen of the amide and amine groups appeared at 399.5 and 401.5 eV, respectively [7]. It was obviously seen from Fig. 2 that the C_{1s} spectra of PU film had the peak of urethane group at 289.1 eV, indicating that there were hard-segment and soft-segment on the PU film surface. For PU-c-CS films, the C_{1s} peak of urethane group at 289.2 eV was also observed, while the C_{1s} spectra of CS film had the peak of ester at 288.8 eV. With increasing degree of ionic complex, the C_{1s} peak of amine and hydroxyl at 286.3 eV depressed while the C_{1s} peaks of C—N bonds at 287.8 eV rose clearly. In N_{1s} peaks, PU, PU-c-CS and CS films showed two peaks at 399.5 and 401.5 eV, respectively. Compared with PU, the strength of the peak of amino group at 401.5 eV of CS was greater sharply. These results confirmed that CS had been immobilized onto the surface of PU.

In our current research, for PTMO-based waterborne PU, the water-swelling ratio changed from 54.6 to 19.8% when the CS content increased from 0 to 12.7% (wt.%) as shown in Table 2. The partly ionized CS and PU could form compact $^{+}H_3N{-}COO^{-}$ layers by electrostatic interactions, which resulted in the formation of PU-c-CS nanoparticles with core–shell structure. Consequently, with CS content increasing, the thicker compact $^{+}H_3N{-}COO^{-}$ layers could induce the films more difficult to swell in water. And the hydrolysis

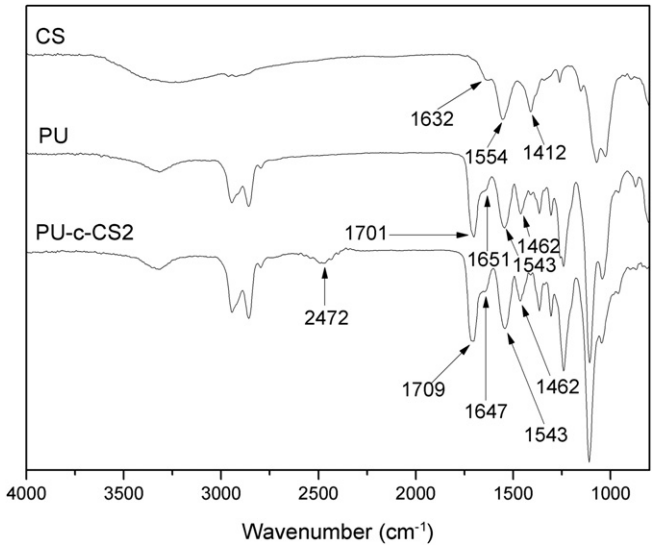

Fig. 2. IR spectra of CS, PU and PU-c-CS films.

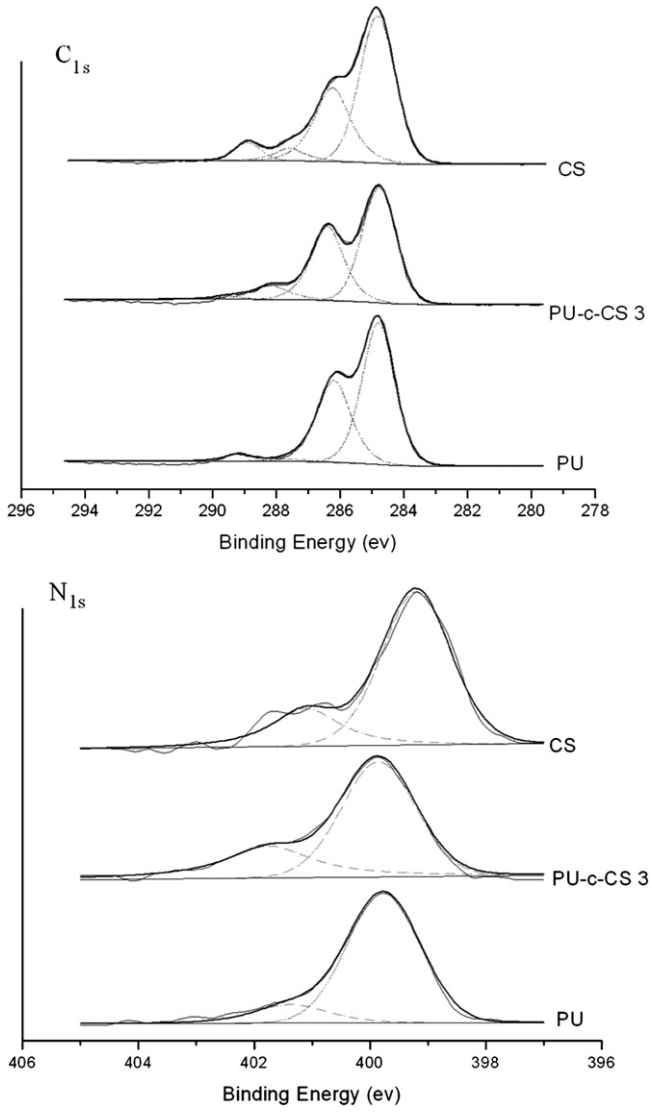

Fig. 3. XPS spectra for C_{1s} and N_{1s} of CS, PU and PU-c-CS films.

weight loss ratio after 48 days was changed from 0.64 to 8.59%. Although modest hydrolysis weight loss happened, most of CS and PU formed the polyelectrolyte complexes.

Table 3 summarized the particle size, polydispersity and ξ-potential of nanoparticles prepared at different CS content. The aggregation was attributed to the formation of clusters caused by ionic bonding between the positively charged $-NH_3^+$ groups of CS and the negatively charged $-COO^-$ groups of PU [38]. The sizes of the emulsion particles increased along with the CS content, and the polydispersity increased with the increase of the particle size. With the addition of CS, more CS was immobilized onto the surface of the PU core by the formation of the CS shell layer through ionic interaction. The diameter of the emulsion particle then increased

Table 2
Sample characterization.

Sample code	Static contact angle (°)	Swelling ratios (%, 24 h)	Loss weight (%, 48 days)
PU	80.1 ± 0.42	54.6	0.64
PU-c-CS1	55.8 ± 0.54	48.5	2.34
PU-c-CS2	46.5 ± 0.21	32.1	6.82
PU-c-CS3	30.7 ± 0.16	19.8	8.59

Table 3
Effective mean diameter, ξ-potential and pH value of PU, PU-c-CS nanoparticles.

Sample	Effective diameter (nm)	Polydispersity	ξ-potential (mV)	pH value
PU	62.2	0.116	−38.8	8.69
PU-c-CS1	89.1	0.182	−29.5	8.13
PU-c-CS2	151.6	0.217	−15.3	7.91
PU-c-CS3	211.1	0.272	7.1	7.78
CS			17.9	6.85

correspondingly. In addition, it was thought that the electrostatic force between anionic PU and cationic CS might play an important role in the change of the particle size in aqueous emulsion. The more CS shell layer was formed, the weaker the restriction power between PU core and CS shell got, and the easier the swelling of CS shell became. These factors could result in the increase of the particle size and polydispersity. The ξ-potential of pure PU aqueous emulsion was negative with ionized carboxylic groups, and the ξ-potential of pure CS solution was positive with ionized amino groups. Similarly, the ξ-potential of emulsion particles increased from an initial value of −38.8 mV to 7.1 mV, and the pH value of aqueous emulsion decreased from 8.69 to 7.78 along with the addition of CS. The fact that ξ-potential increased more than mathematical calculations, suggested that CS be in the outermost layer of the particles.

Fig. 4 showed the TEM photographs of PU and PU-c-CS nanoparticles. Fig. 4A obviously showed that the PU nanoparticles were spherical. In the case of dropping CS solution into PU aqueous emulsion, PU-c-CS nanoparticles were formed by ionic interaction between cationic CS and anionic PU at the PU spherical surfaces [38]. The PU core had been initially generated, and the CS coacervate layer was formed on the surface of PU core. The high-magnification image (Fig. 4B) clearly displayed PU-c-CS nanoparticles had core–shell structure. And the formed PU-c-CS interface complex layer prevented more CS solution to diffuse into the core to further complex with PU. The dimension and size distribution of the nanoparticles shown in Fig. 4 were also consistent with the results determined by DLS.

All the emulsions exhibited satisfactory stability in the whole range of the testing temperature from the freeze–thaw test. Though the size of the emulsion particles increased, the aqueous emulsions were stable owing to hydrophilic groups such as CS and carboxylic anions.

3.2. Film general characterization

The surface morphologies of PU and PU-c-CS films were monitored by AFM in tapping mode and were displayed in Fig. 5A and B, respectively. The PU films were very smooth, and the drop height of the surface was 12.7 nm. The PU-c-CS film was rougher than the PU film, and the drop height of the surface was 23.0 nm. The average roughness (RMS) was calculated from AFM images, 0.67 nm for PU and 2.96 nm for PU-c-CS2, respectively. The AFM images (shown in Fig. 5A and C) exhibited the light and dark micro-regions around 100 nm, which were the specific microphase-separated morphologies, consisting of hard-segment-rich and soft-segment-rich domains. Besides the small light and dark micro-regions, there were many big light spherical bodies with the dimension around 200 nm (shown in Fig. 5B and D). CS was viewed as hard composition, and hard-segment-rich domains of the PU-c-CS films would be increased with the addition of CS. From the molecule geometric arrangement point of view, it was definitely that the increase of CS would lead to the increase in the number of the hard segments, and, therefore, the average size of hard domains increased correspondingly. The light regions in phase image correspond to hard-segment-rich domains and the dark regions correspond to soft-segment-rich domains. So these big light regions could be assigned to the domains of PU coated by CS.

The results from Table 2 showed that the samples became more hydrophilic after the addition of CS. As a result, the contact angles decreased from 80.1° to 30.7° when the CS content increased from 0 to 12.7% (wt.%). It was ascribed to the introduction of hydrophilic groups in CS, and the hydrophobic PU core surrounded by the hydrophilic CS coat shown in Fig. 1 and Fig. 4B.

The results of General Tensile Test (Table 4) demonstrated that the films showed good mechanical properties. It was attributed to

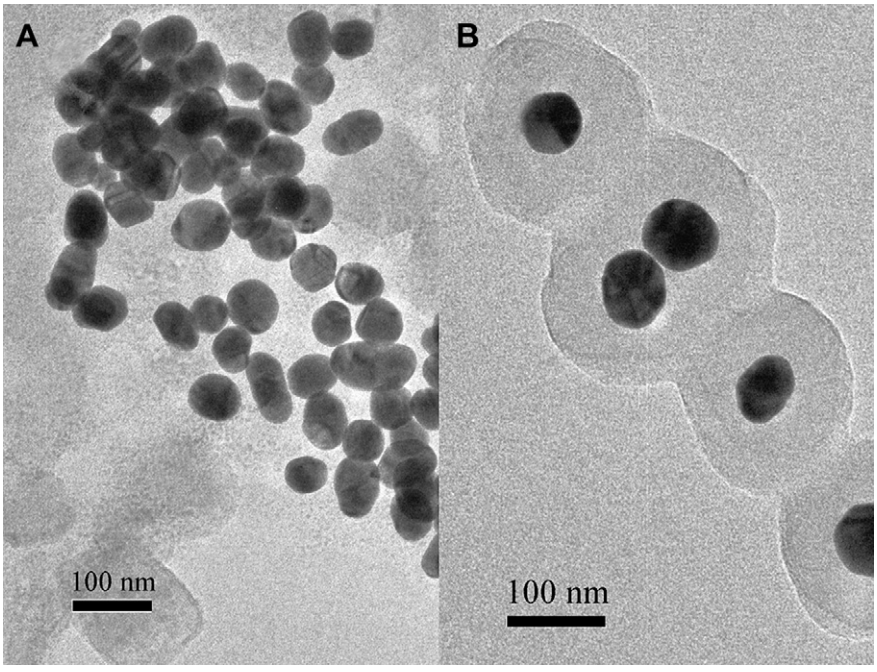

Fig. 4. The TEM photographs of PU and PU-c-CS nanoparticles: (A) PU, and (B) PU-c-CS2.

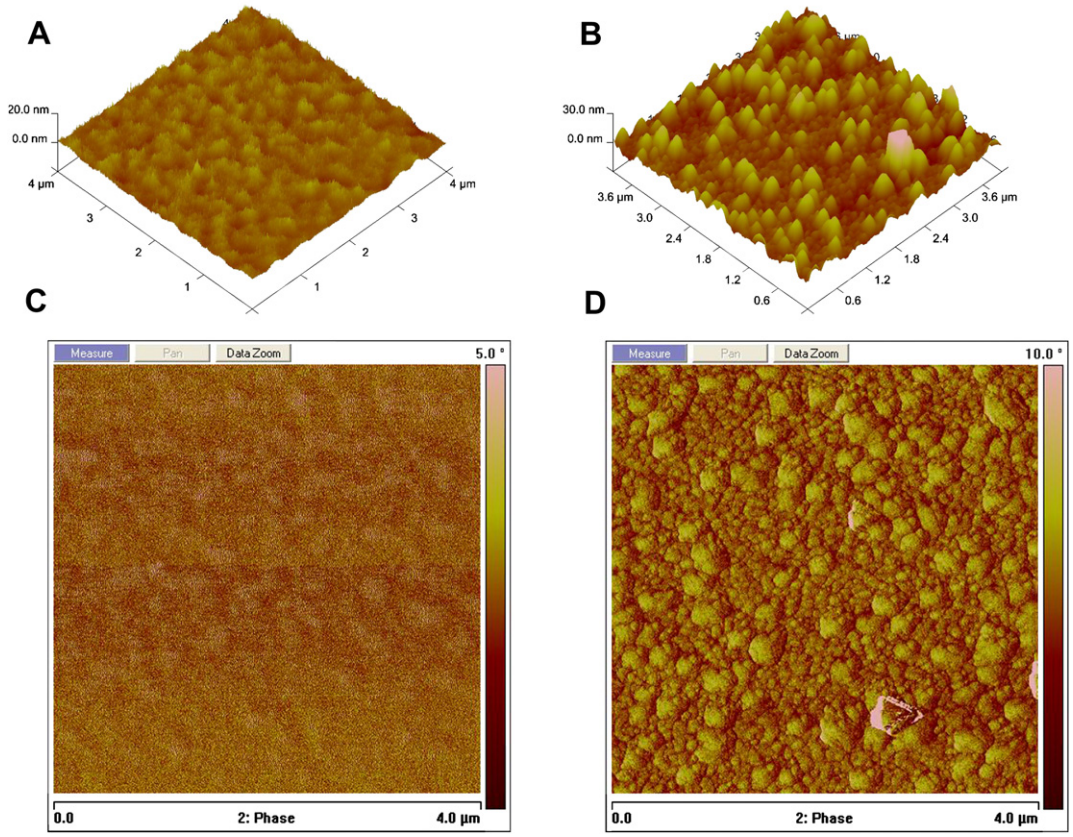

Fig. 5. The AFM images to present the surface morphology of the PU and PU-c-CS films: (A) 3D image of PU, (B) 3D image of PU-c-CS2, (C) phase image of PU, and (D) phase image of PU-c-CS2.

specific microphase-separated morphology of the PU scaffolds, which consisted of hard-segment-rich and soft-segment-rich domains (Fig. 5C and D). And with the increase of the CS content, Young's modulus increased greatly from 41.7 Mpa to 149.5 Mpa, while the elongation of strain decreased sharply from 847.3% to 108.5%. It could be explained that in block PU, soft segments contributed to the elasticity and low-temperature properties, whereas the hard segments contributed to the modulus, strength, and elevated temperature properties [30]. CS was rigid molecule, which provided materials with high modulus strength. Thus the addition of CS could be viewed as increasing of total hard compositions in PU-c-CS. The above-mentioned results were consistent with the morphology of the films in Fig. 5. Hence, Young's modulus increased in the order of PU < PU-c-CS1 < PU-c-CS2 < PU-c-CS3, while the elongation of strain decreased in the order of PU > PU-c-CS1 > PU-c-CS2 > PU-c-CS3.

3.3. Biological properties of the materials

ECV304 endothelial cells were cultured on the surface of CS, PU films, PU-c-CS films and Petri dish (polystyrene) as control, respectively. Cell density was indirectly determined by hemocytometer and MTT assay at 12, 24, 48, 72 and 96 h, and the data were given in Fig. 6. The results showed that there was significant difference about ECV304 endothelial cell density on the PU film and CS film, especially after 48 h of incubation, suggesting that CS film facilitate the growth of ECV304 endothelial cell. These results also demonstrated that the hydrophobicity and the intrinsic inert

Table 4
General of tensile test of PU and PU-c-CS films.

Sample	Percent strain at peak (%)	Young's modulus (MPa)	Stress at break (Mpa)
PU	847.333	41.769	30.865
PU-c-CS1	653.567	62.810	28.371
PU-c-CS2	335.200	111.881	17.993
PU-c-CS3	108.567	149.558	15.373

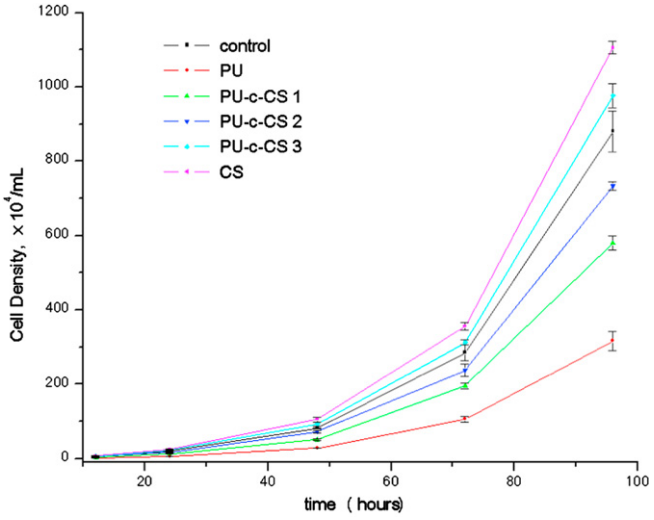

Fig. 6. ECV304 cell proliferation analysis after cultured for different time in a humidified air containing 5% CO_2 at 37 °C on the surface of control, PU, PU-c-CS1, PU-c-CS2, PU-c-CS3 and CS, respectively. Cell seeding density is 1.0×10^5/ml.

properties of PU were not favorable for the cell growth and spreading. By comparing the results of the cell density between the PU-c-CS films and PU film after 12 h and 96 h, the cell density on PU-c-CS films obviously increased with the enhancement of CS content. This was consistent with the results observed by Yang et al. [16]. The increase of the surface hydrophilicity and immobilization of biocompatible CS provided the possibility to enhance the interaction between cells and PU-c-CS films. It would be favorable for the promotion of cell attachment and proliferation [3]. Therefore, these CS-immobilized PU films proved to be non-cytotoxic and could support cell adhesion and growth.

The morphology of ECV304 endothelial cells on CS, PU film, PU-c-CS films, and polystyrene as control were examined under light microscopy and the microscopic observations after 12, 24, 48 and 72 h of seeding (Fig. 7). It could be seen from the figure that ECV304 endothelial cells on PU film and CS film were round and with limited or no attachment to the cells. They were able to be easily removed by medium and floated in the medium. By comparing the morphology of cells on CS film and PU film, it was showed that the cells on CS film were highly transparent, while the cells on PU film appeared as dark particles within cells and cell fragments increased a little after 12 h of culture. These observations revealed that CS film not only remained as cells viable but also benefited the cell proliferation, and demonstrated that CS, natural polysaccharide, had better biocompatibility than that of synthetic PU, even though both PU film and CS film were shown to be poorly adhering substrates. When the cells were cultured on PU-c-CS films, the morphology of ECV304 endothelial cells had significant difference from that of PU film or CS film. The cells on PU-c-CS2 film appeared highly transparent, attached and well spread after cultured for 12 h similar to the cells on the control of polystyrene, suggesting that PU-c-CS2 film did help ECV304 endothelial cells to retain their phenotype.

The cell adhesion to artificial substrate was usually affected by surface charge, biological and chemical properties of molecules on the substrate surface and also the molecular aggregation form on the surface, etc., [14,39]. From the results of our experiment, either PU film with negative charge and hydrophobicity or CS film with positive charge was not favorable for the cell attachment and spreading. It was reasonable to assume that there were suitable charge, hydrophobic domain and hydrophilic domain on the surface of PU-c-CS films which could facilitate the cell adhesion and proliferation. Therefore, CS immobilization onto the surface of PU was possible to promote the endothelium regeneration of vascular scaffold [3].

Plasma protein adsorption was one of the most important phenomena in determination of the biocompatibility of the implantable materials [32]. The amounts of BSA protein adsorption on the surface of PU, PU-c-CS1, PU-c-CS2 and PU-c-CS3 were 387.98 ± 4.56, 273.65 ± 10.79, 215.05 ± 5.25, and 161.14 ± 5.06 μg/mL, respectively. According to an earlier report, hydrophobic surface was favorable to protein adsorption [40]. Increasing hydrophilicity of the surfaces was commonly used for the reduction of non-specific protein adsorption to biomaterials surfaces. The report indicated that the amount of BSA protein adsorbed on the film surface increased while the water contact angle increased. Our experimental data were consistent with the report. PU exhibited high adsorption of BSA protein, and the adsorbed amount of protein decreased after CS immobilization onto PU films. With the addition of CS, the hydrophilicity of the PU–CS surfaces increased, whilst the adsorption of proteins decreased.

The blood coagulation cascade included intrinsic pathway, extrinsic pathway, and common pathway. APTT and PT are used to mainly examine the intrinsic and common pathway [34,35]. Table 5 showed that the *in vitro* anticoagulation activity of samples with the clotting time as readout. The PT of all samples was almost the same level, which indicated that both PU film and PU-c-CS films could not restrain the prothrombin activity separately. The APTT of the PU film was 35.6 ± 0.31 (s), which was similar to other's study of PU films [41]. After PU film was modified by CS, the results showed

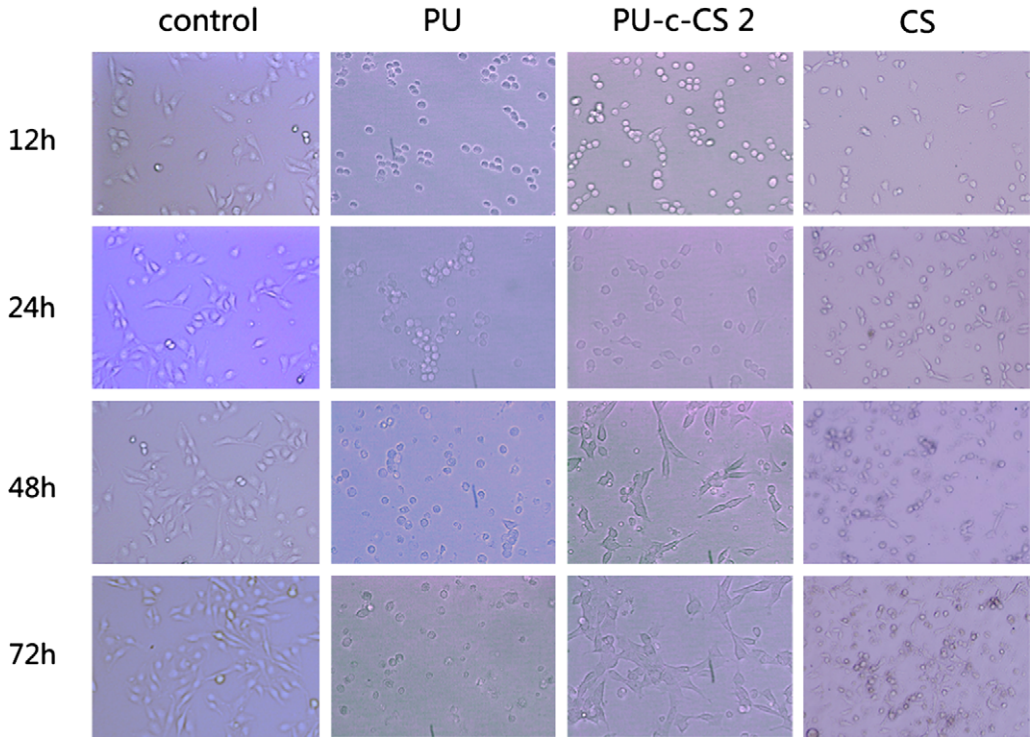

Fig. 7. Microscopy photographs of ECV304 cells at 12, 24, 48, 72 h after they were plated on polystyrene control, PU, PU-c-CS2 and CS films.

Table 5
The anticoagulant ability of PU and PU-c-CS films.

Sample	The recalcification test			Anticoagulation time	
	RT (s)	t_{sample}/t_{black}	t_{sample}/t_{SO}	APTT (s)	PT (s)
Black	32.7 ± 2.49		0.64	40.2 ± 0.37	11.6 ± 0.05
Silicon oil (SO)	51.3 ± 7.01	1.57			
PU	45.1 ± 4.86	1.38	0.88	35.6 ± 0.31	11.4 ± 0.07
PU-c-CS1	46.4 ± 5.57	1.42	0.90	91.6 ± 0.59	11.7 ± 0.12
PU-c-CS2	67.4 ± 11.5	2.06	1.31	126.9 ± 0.87	11.9 ± 0.11
PU-c-CS3	78.1 ± 13.9	2.39	1.52	147.2 ± 1.31	12.3 ± 0.19

that the APTT of PU-c-CS film increased with the content of CS and the APTT of PU-c-CS3 film was prolonged more than 4 times than that of PU film, suggesting that the good anticoagulation activity of PU-c-CS films could be achieved. The reason of this change was that CS showed little hemostatic effect, and exhibited the anti-coagulation property of the whole blood [42]. In our work, the APTT of CS, natural heparin-like glycosaminoglycan, was more than 320 s (upper limit of the automated blood coagulation analyzer). On the other hand, blood compatibility was evaluated by the recalcification time. The blank tubes and the tubes coated with silicon oil were as control. The recalcification time of the blank tubes was 32.7 ± 2.49 s and that of tubes coated with silicon oil was 51.3 ± 7.01 s. The recalcification time ratios of the tube coated with the samples to the blank tube and to the tube coated with silicon oil were shown in Table 5. It could be seen that the blood compatibility also increased in the order of PU < PU-c-CS1 < PU-c-CS2 < PU-c-CS3, which was consistent with the result of the APTT. Through the immobilization of CS onto the surface of PU film, the heparin-like structure was formed, which could have the structure of anti-thrombin-binding region and suppress platelet adhesion onto films, and improved hemocompatibility of PU films [43].

4. Conclusions

The core–shell structure of PU-c-CS was formed in aqueous emulsion through electrostatic interaction of oppositely charged polyelectrolytes, and CS was subsequently immobilized onto the PU surface. The PU-c-CS aqueous emulsions exhibited satisfactory stability and were green to environment, which could widely be used due to its good processability and very mild formation conditions. The structures were confirmed by IR, XPS, DLS, TEM and AFM. The remarkable advantage of this structure was to combine the biological and mechanical properties of CS and PU. The CS-immobilized PU films favored for cells adhesion and growth, reduced plasma protein adsorption, and improved hemocompatibility, whilst good mechanical properties were reserved. Hence, PU-c-CS materials could provide a new candidate for implantable materials.

Acknowledgements

We gratefully acknowledge Prof. J. L. Fang and Prof. Z. R. Yuan for the use of FTIR and DSC equipments. And the technical assistance from Prof. Liu Z. H. of Department of Biochemistry is also acknowledged for TEM.

Appendix. Supplementary material

Supplementary material can be found, in the online version, at doi:10.1016/j.polymer.2010.03.008.

References

[1] Silva SS, Menezes SMC, Garcia RB. Eur Polym J 2003;39:1515–9.
[2] Yuan YL, Ai F, Zang XP, Zhuang W, Shen J, Lin SC. Colloid Surf B 2004;35:1–5.
[3] Zhu YB, Gao CY, He T, Shen JC. Biomaterials 2004;25:423–30.
[4] Puskas JE, Chen YH. Biomacromolecules 2004;5:1141–54.
[5] Ajili SH, Ebrahimi NG, Khorasani MT. J Appl Polym Sci 2003;89:2496–501.
[6] Ma ZW, Gao CY, Ji JA, Shen JC. Eur Polym J 2002;38:2279–84.
[7] Guan JJ, Gao CY, Feng LX, Shen JC. Eur Polym J 2000;36:2707–13.
[8] Guan JJ, Gao CY, Feng LX, Sheng JC. J Biomater Sci Polym Ed 2000;11:523–36.
[9] Ko YG, Kim YH, Park KD, Lee HJ, Lee WK, Park HD, et al. Biomaterials 2001;22:2115–23.
[10] Guan JJ, Gao CY, Feng LX, Shen JC. J Mater Sci Mater Med 2001;12:447–52.
[11] Suh H, Hwang YS, Lee JE, Han CD, Park JC. Biomaterials 2001;22:219–30.
[12] Zhu HG, Ji J, Lin RY, Gao CY, Feng LX, Shen JC. Biomaterials 2002;23:3141–8.
[13] Black FE, Hartshorne M, Davies MC, Roberts CJ, Tendler SJB, Williams PM, et al. Langmuir 1999;15:3157–61.
[14] Ding Z, Chen JN, Gao SY, Chang JB, Zhang JF, Kang ET. Biomaterials 2004;25:1059–67.
[15] Lin WC, Tseng CH, Yang MC. Macromol Biosci 2005;5:1013–21.
[16] Yang JM, Yang SJ, Lin HT, Wu TH, Chen HJ. Mater Sci Eng C Biomimetic Supramolecular Systems 2008;28:150–6.
[17] Muzzarelli RAA. Chitin. Oxford: Pergamon Press; 1977.
[18] Uragami T, Tokura S. Material science of chitin and chitosan. New York: Springer; 2006.
[19] Kumar MNVR, Muzzarelli RAA, Muzzarelli C, Sashiwa H, Domb AJ. Chem Rev 2004;104:6017–84.
[20] Chandy T, Sharma C. Biomater Artif Cells Artif Organs 1990;18:1–24.
[21] Muzzarelli RAA. Carbohydr Polym 1993;20:7–16.
[22] Muzzarelli RAA, Mattioli-Belmonte M, Tietz C, Biagini R, Ferioli G, Brunelli MA, et al. Biomaterials 1994;15:1075–81.
[23] Rutnakornpituk M, Ngamdee P, Phinyocheep P. Polymer 2005;46:9742–52.
[24] Mori T, Okumura M, Matsuura M, Ueno K, Tokura S, Okamoto Y, et al. Biomaterials 1997;18:947–51.
[25] Ueno H, Yamada H, Tanaka I, Kaba N, Matsuura M, Okumura M, et al. Biomaterials 1999;20:1407–14.
[26] Chupa JM, Foster AM, Sumner SR, Madihally SV, Matthew HWT. Biomaterials 2000;21:2315–22.
[27] Suh JKF, Matthew HWT. Biomaterials 2000;21:2589–98.
[28] Xu D, Meng Z, Han M, Xi K, Jia XD, Yu XH, et al. J Appl Polym Sci 2008;109:240–6.
[29] Yuan XY, Sheng J, He F, Tang Y, Shen NX. J Appl Polym Sci 1998;69:1907–15.
[30] Chen H, Jiang XW, He L, Zhang T, Xu M, Yu XH. J Appl Polym Sci 2002;84:2474–80.
[31] Yang JM, Shih CH, Chang CN, Lin FH, Jiang JM, Hsu YG, et al. J Biomed Mater Res Part A 2003;64A:138–46.
[32] Kwon MJ, Bae JH, Kim JJ, Na K, Lee ES. Int J Pharm 2007;333:5–9.
[33] Nagahama K, Nishimura Y, Ohya Y, Ouchi T. Polymer 2007;48:2649–58.
[34] Osoniyi O, Onajobi FJ. Ethnopharmacol 2003;89:101–5.
[35] Campos ITN, Tanaka-Azevedo AM, Tanaka AS. FEBS Lett 2004;577:512–6.
[36] Cha JN, Birkedal H, Euliss LE, Bartl MH, Wong MS, Deming TJ, et al. J Am Chem Soc 2003;125:8285–9.
[37] Hu Y, Chen Y, Chen Q, Zhang LY, Jiang XQ, Yang CZ. Polymer 2005;46:12703–10.
[38] Hu Y, Jiang XQ, Ding Y, Chen Q, Yang CZ. Adv Mater 2004;16:933–7.
[39] Chatelet C, Damour O, Domard A. Biomaterials 2001;22:261–8.
[40] Tangpasuthadol V, Pongchaisirikul N, Hoven VP. Carbohydr Res 2003;338:937–42.
[41] Lv Q, Cao CB, Zhu HS. J Mater Sci Mater Med 2004;15:607–11.
[42] Lin CW, Lin JC. Biomacromolecules 2003;4:1691–7.
[43] Björk I, Lindahl U. Mol Cell Biochem 1982;48:161–82.